Structural Identifiability Analysis of a Cardiovascular System Model [☆,☆☆]

Antoine Pironet[a,*], Pierre C. Dauby[a], J. Geoffrey Chase[b], Paul D. Docherty[b], James A. Revie[b], Thomas Desaive[a]

[a] *University of Liège (ULg), GIGA-Cardiovascular Sciences, Liège, Belgium*
[b] *University of Canterbury, Department of Mechanical Engineering, Christchurch, New Zealand*

Abstract

The six-chamber cardiovascular system model of Burkhoff and Tyberg has been used in several theoretical and experimental studies. However, this cardiovascular system model (and others derived from it) are not identifiable from any output set.

In this work, two such cases of structural non-identifiability are first presented. These cases occur when the model output set only contains a single type of information (pressure or volume).

A specific output set is thus chosen, mixing pressure and volume information and containing only a limited number of clinically available measurements. Then, by manipulating the model equations involving these outputs, it is demonstrated that the six-chamber cardiovascular system model is structurally globally identifiable.

A further simplification is made, assuming known cardiac valve resistances. Because of the poor practical identifiability of these four parameters, this assumption is usual. Under this hypothesis, the six-chamber cardiovascular system

[☆] Word count: 4050.
[☆☆] Abbreviation: CVS (cardiovascular system).

Preprint submitted to Elsevier *December 21, 2015*

[*] Corresponding author. *Phone:* +32 4 366 33 56
Email address: a.pironet@ulg.ac.be (Antoine Pironet)

model is structurally identifiable from an even smaller dataset.

As a consequence, parameter values computed from limited but well-chosen datasets are theoretically unique. This means that the parameter identification procedure can safely be performed on the model from such a well-chosen dataset. The model is thus fully suitable to be used for diagnosis.

Keywords: Identifiability; parameter identification; lumped-parameter model; physiological model.

1. Introduction

1.1. Background

Accurately determining cardiac parameters in the intensive care unit is difficult since only indirect data of the patient's cardiovascular state is available and this state is also rapidly changing. Mathematical models of the cardiovascular system (CVS) have been developed to provide clinicians with additional information regarding the overall picture of the cardiac and circulatory state. To be clinically relevant, these models have to be patient-specific, which means that their parameters have to be identified so that simulations represent a patient's individual state. This task is not obvious due to the indirect nature of the necessary clinical data.

The CVS can be modelled using very different approaches, including finite element models [1], pulse-wave propagation models [2], and lumped-parameter models [3]. The present study focuses on one such lumped-parameter model. Lumped-parameter models represent whole sections of the CVS as single elements (chambers or resistances, for example). An important advantage of these models is that they have few parameters, and thus, these parameters can be more readily identified from clinical data. The main drawback of lumped-parameter models is that they cannot be used to gain local spatial information on the CVS.

The CVS model used in this work has been developed by Burkhoff and Tyberg [3]. It is a simple lumped-parameter model that describes the whole CVS using six state equations and thirteen parameters (*cf.* Figure 1). This model is the simplest model to consider systemic and pulmonary circulations. This model has allowed theoretical studies assessing the consequences of left ventricular dysfunction [3] and ventricular interaction [4].

From an experimental point of view, a similar model has been used for hemodynamic monitoring during septic shock [5] and pulmonary embolism [6, 7]. The model parameters, such as systemic and pulmonary vascular resistances, ventricular end-systolic elastances and pulmonary arterial elastance, are needed by clinicians to assess the severity of a condition. The model has also recently been used to compute total stressed blood volume [8], an index of fluid responsiveness [9]. Furthermore, many other models, more complex, can be seen as extensions of this simple model [4, 10–13]. One of these more complex models has been used to investigate the haemodynamic state of patients after mitral valve replacement surgery [14].

However, as will be shown further, there are several measurement sets from which the parameters of this model (and other models derived from it) cannot be uniquely computed. The key question is: *can we find a measurement set which allows to identify all model parameters?* In more theoretical terms, this

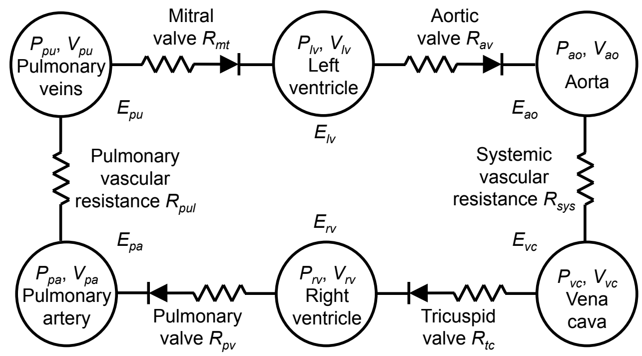

Figure 1: Schematic representation of the six-chamber CVS model.

question can be stated as: *what is the set of model outputs one has to include in the model definition for this model to be structurally globally identifiable?* This notion of structural identifiability is defined in the next subsection.

1.2. Structural identifiability

Structural identifiability analysis of a model determines whether all model parameters can be uniquely retrieved in the perfect conditions of noise-free and continuous measurements of the model outputs. If the answer is yes, then the model is said to be *structurally globally identifiable* [15, 16]. Otherwise, if there exists multiple parameter values for the given model outputs, the model is *structurally locally identifiable*. Finally, if there is an infinite number of possible parameter values, the model is termed *structurally non-identifiable*.

Structural identifiability is called *structural* because it only depends on the model equations (its *structure*). Thus, it depends on the roles of the parameters and the nature and number of the available model outputs. For instance, if the number of model outputs is too low, the model is likely to be non-identifiable.

Taking the measurement noise and the practically finite number of data points into account and investigating if the model parameters still can be uniquely determined relates to a different topic, called *practical identifiability* [17]. The tools used to investigate practical identifiability are different and include, for instance, sensitivity analyses and parameter correlation analyses [8]. Structural identifiability is a necessary condition for practical identifiability. It is therefore risky to perform a parameter identification procedure on a model which has not been shown to be structurally identifiable.

1.3. Goal

This work aims to prove the structural identifiability of the CVS model from a clinically available output set. As said above, this structural identifiability analysis is a necessary step to ensure that results obtained when identifying the model parameters from limited clinical data are unique, and thus, relevant.

2. Methods

2.1. Six-chamber cardiovascular system model

The CVS model that is the focus of this work has been previously presented by Burkhoff and Tyberg [3] and is shown in Figure 1. The model comprises six elastic chambers linked by resistive vessels. These six chambers represent the aorta, the vena cava, the pulmonary artery, the pulmonary veins ($i = ao$, vc, pa and pu) and the two ventricles ($i = lv$ and rv).

The arterial and venous chambers are modelled as passive chambers with a constant linear relationship between pressure P_i and (stressed) volume V_i:

$$P_{ao}(t) = E_{ao} \cdot V_{ao}(t) \tag{1}$$

$$P_{vc}(t) = E_{vc} \cdot V_{vc}(t) \tag{2}$$

$$P_{pa}(t) = E_{pa} \cdot V_{pa}(t) \tag{3}$$

$$P_{pu}(t) = E_{pu} \cdot V_{pu}(t) \tag{4}$$

where the constant parameters E_i are called the elastances of the chambers.

Ventricular chambers are active. Thus, the relationship between pressure and volume is time-varying [18]:

$$P_{lv}(t) = E_{lv} \cdot e_{lv}(t) \cdot V_{lv}(t) \tag{5}$$

$$P_{rv}(t) = E_{rv} \cdot e_{rv}(t) \cdot V_{rv}(t). \tag{6}$$

In Equations (5) and (6), the constant parameters E_{lv} and E_{rv} are the end-systolic elastances and the functions $e_{lv}(t)$ and $e_{rv}(t)$ are called the driver functions. These driver functions can take different forms, but for the model to correctly mimic the physiological activity of the normal heart, $e_{lv}(t)$ and $e_{rv}(t)$ have (at least) to be periodic with period T (the cardiac period), range from 0 (diastole) to 1 (end-systole) and rise and fall at approximately the same time. Equally, it has been shown that while this approach still holds in disease, there are subtle changes to driver functions based on disease sate [19]. Also note that, for simplicity, no end-diastolic pressure-volume relationships were inserted in Equations (5) and (6).

The six chambers are linked by resistive vessels, representing the four heart valves (mitral: mt, aortic: av, tricuspid: tc and pulmonary: pv) and the systemic and pulmonary circulations (sys and pul). In these last two vessels, flow Q is given by Ohm's law:

$$Q_{sys}(t) = \frac{P_{ao}(t) - P_{vc}(t)}{R_{sys}} \tag{7}$$

$$Q_{pul}(t) = \frac{P_{pa}(t) - P_{pu}(t)}{R_{pul}}, \tag{8}$$

where R_{sys} (respectively R_{pul}) denotes the total resistance of the systemic (respectively pulmonary) circulation. In the case of the valves, the model assumes that there is only flow when the pressure difference across the valve is positive. Hence, one has:

$$Q_{mt}(t) = \frac{1}{R_{mt}} \begin{cases} P_{pu}(t) - P_{lv}(t) & \text{if } P_{pu}(t) > P_{lv}(t) \\ 0 & \text{otherwise} \end{cases} \tag{9}$$

$$Q_{av}(t) = \frac{1}{R_{av}} \begin{cases} P_{lv}(t) - P_{ao}(t) & \text{if } P_{lv}(t) > P_{ao}(t) \\ 0 & \text{otherwise} \end{cases} \tag{10}$$

$$Q_{tc}(t) = \frac{1}{R_{tc}} \begin{cases} P_{vc}(t) - P_{rv}(t) & \text{if } P_{vc}(t) > P_{rv}(t) \\ 0 & \text{otherwise} \end{cases} \tag{11}$$

$$Q_{pv}(t) = \frac{1}{R_{pv}} \begin{cases} P_{rv}(t) - P_{pa}(t) & \text{if } P_{rv}(t) > P_{pa}(t) \\ 0 & \text{otherwise.} \end{cases} \tag{12}$$

Finally, volume change in any of the model chambers is dictated by the difference between flow going in and coming out of the chamber:

$$\dot{V}_{lv}(t) = Q_{mt}(t) - Q_{av}(t) \tag{13}$$

$$\dot{V}_{ao}(t) = Q_{av}(t) - Q_{sys}(t) \tag{14}$$

$$\dot{V}_{vc}(t) = Q_{sys}(t) - Q_{tc}(t) \tag{15}$$

$$\dot{V}_{rv}(t) = Q_{tc}(t) - Q_{pv}(t) \tag{16}$$

$$\dot{V}_{pa}(t) = Q_{pv}(t) - Q_{pul}(t) \tag{17}$$

$$\dot{V}_{pu}(t) = Q_{pul}(t) - Q_{mt}(t). \tag{18}$$

Summing Equations (13) to (18) gives:

$$\begin{aligned} &\dot{V}_{lv}(t) + \dot{V}_{ao}(t) + \dot{V}_{vc}(t) \\ &+ \dot{V}_{rv}(t) + \dot{V}_{pa}(t) + \dot{V}_{pu}(t) = 0 \end{aligned} \tag{19}$$

and integrating Equation (19) yields:

$$\begin{aligned} &V_{lv}(t) + V_{ao}(t) + V_{vc}(t) \\ &+ V_{rv}(t) + V_{pa}(t) + V_{pu}(t) = \text{SBV}. \end{aligned} \tag{20}$$

Equation (19) expresses the fact that, since the model is a closed-loop, there is no flow going in or out of the whole CVS. Equation (20) expresses that, as a consequence, total (stressed) blood volume in the model is a constant. This constant volume value is denoted SBV and represents another model parameter.

The model parameter set $\mathbf{p}$ thus consists of thirteen elements:

$$\begin{aligned} \mathbf{p} = \quad &(E_{ao}\ E_{vc}\ E_{pa}\ E_{pu}\ E_{lv}\ E_{rv} \\ &R_{sys}\ R_{pul}\ R_{mt}\ R_{av}\ R_{tc}\ R_{pv}\ \text{SBV}). \end{aligned} \tag{21}$$

Several examples of parameter identification procedures performed on this model and based on actual measurements are available in the literature [5–8, 13, 14].

2.2. Output sets

In this section, three different output sets $\mathbf{y}^k$ ($k = 1$, 2 or 3) are proposed for this model. Structural identifiability of the model is then assessed for each of these output sets.

2.2.1. Output set containing only volumes

To show a first example of structural non-identifiability, it is assumed that all chamber volumes are model outputs. Consequently, the outputs of the six-chamber model are:

- volume in the aorta $V_{ao}(t)$,
- volume in the pulmonary artery $V_{pa}(t)$,
- volume in the vena cava $V_{vc}(t)$,
- volume in the pulmonary veins $V_{pu}(t)$,
- volume in the left ventricle $V_{lv}(t)$ and
- volume in the right ventricle $V_{rv}(t)$.

and the output set is

$$\mathbf{y}^1 = \left(V_{ao}(t)\ V_{pa}(t)\ V_{vc}(t)\ V_{pu}(t)\ V_{lv}(t)\ V_{rv}(t)\right). \tag{22}$$

2.2.2. Output set containing only pressures

For the second example of structural non-identifiability, it is assumed that all chamber pressures are model outputs. Consequently, the outputs of the six-chamber model are:

- pressure in the aorta $P_{ao}(t)$,
- pressure in the pulmonary artery $P_{pa}(t)$,
- pressure in the vena cava $P_{vc}(t)$,
- pressure in the pulmonary veins $P_{pu}(t)$,
- pressure in the left ventricle $P_{lv}(t)$ and
- pressure in the right ventricle $P_{rv}(t)$

and the output set is:

$$\mathbf{y}^2 = \left(P_{ao}(t)\ P_{pa}(t)\ P_{vc}(t)\ P_{pu}(t)\ P_{lv}(t)\ P_{rv}(t)\right). \tag{23}$$

2.2.3. Clinically available output set

Finally, to show structural identifiability, the outputs of the six-chamber model are chosen to be the following clinically available measurements:

- pressure in the aorta $P_{ao}(t)$,
- pressure in the pulmonary artery $P_{pa}(t)$,
- pressure in the vena cava $P_{vc}(t)$,
- pressure in the pulmonary veins $P_{pu}(t)$ and
- stroke volume SV.

Stroke volume is defined as the volume of blood ejected by the heart each time it beats. It is thus a scalar quantity. At steady state, left and right ventricular stroke volumes are equal. The availability of these measurements in a clinical setting is explained in Section 4. The output set now reads:

$$\mathbf{y}^3 = (P_{ao}(t)\ P_{pa}(t)\ P_{vc}(t)\ P_{pu}(t)\ \mathrm{SV}). \tag{24}$$

2.3. Figures

In the next section, theoretical results are presented, which are valid for any non-trivial value of the model parameters $\mathbf{p}$, and any driver functions $e_{lv}(t)$ and $e_{rv}(t)$ respecting the conditions described in Section 2.1. To provide an illustration of the theoretical results, several figures are also presented. The generation of such figures required choosing a particular error metric and particular parameter values, as described in this section. As previously stated, these choices only relate to the generation of the figures, while the results presented remain completely general.

2.3.1. Error vector

To illustrate the results, an error vector $\mathbf{e}^k$ is defined, representing the relative difference between references $\mathbf{y}^k(t)$ and simulations $\hat{\mathbf{y}}^k(\mathbf{p}, t)$ of the output over one cardiac period T:

$$e_i^k(\mathbf{p}, t) = \frac{y_i^k(t) - \hat{y}_i^k(\mathbf{p}, t)}{y_i^k(t)} \text{ for } 0 \leq t < T. \tag{25}$$

2.3.2. Error function

Then, a scalar error function ψ^k is defined as the integral over one cardiac period of the sum of the squared components of $\mathbf{e}^k$:

$$\psi^k(\mathbf{p}) = \int_0^T \sum_i [e_i^k(\mathbf{p}, t)]^2 \, dt. \tag{26}$$

This scalar error function ψ^k is represented in the figures of the next section.

2.3.3. Reference outputs

In this work, since the focus is set on *structural* identifiability, the data used is assumed to be perfect, in other words, noise-free and continuous. To remain as close as possible to this hypothesis, the reference curves $\mathbf{y}^k$ required for illustration are obtained from model simulations with a given parameter set $\mathbf{p}^*$. The goal of the procedure is to investigate whether or not a different parameter set $\mathbf{p}^\dagger$ can lead to the same curves.

The reference parameter set $\mathbf{p}^*$ can be arbitrarily chosen, since it is only necessary for illustrative purposes. It was obtained from a previously published study on the same model [8]. The simulation also required specific driver functions to be chosen, more precisely [8]:

$$e_{lv}(t) = e_{rv}(t) = \exp\left[-80(t \bmod 0.6) - 0.3)^2\right], \tag{27}$$

where t is expressed in seconds and mod denotes the modulo operator.

3. Results

As previously mentioned, there are certain measurement sets from which the model parameters cannot be uniquely determined. In these cases, the model is structurally non-identifiable. Two such cases are first described in this section.

3.1. Output set containing only volumes

From the model equations, it can be seen that all simulated volumes will be exactly the same if all elastances (E_{ao}, E_{vc}, E_{pa}, E_{pu}, E_{lv} and E_{rv}) and resistances (R_{sys}, R_{pul}, R_{mt}, R_{av}, R_{tc}, R_{pv}) are multiplied by the same factor. Indeed, expressing Equations (13) to (18) solely in terms of volumes by substituting pressures and flows using Equations (1) to (12) shows that equations linking volume derivatives to volumes only involve the following ratios of elastances to resistances:

$$\frac{E_{pu}}{R_{mt}}, \frac{E_{lv}}{R_{mt}}, \frac{E_{lv}}{R_{av}}, \frac{E_{ao}}{R_{av}}, \frac{E_{ao}}{R_{sys}}, \frac{E_{vc}}{R_{sys}}, \frac{E_{vc}}{R_{tc}}, \frac{E_{rv}}{R_{tc}}, \frac{E_{rv}}{R_{pv}}, \frac{E_{pa}}{R_{pv}}, \frac{E_{pa}}{R_{pul}}, \frac{E_{pu}}{R_{pul}}. \tag{28}$$

As an illustration, Figure 2 shows that the error function ψ^1 is identically zero all along the line $a = b$, where a is a factor multiplying all the elastances and b is one multiplying all the resistances.

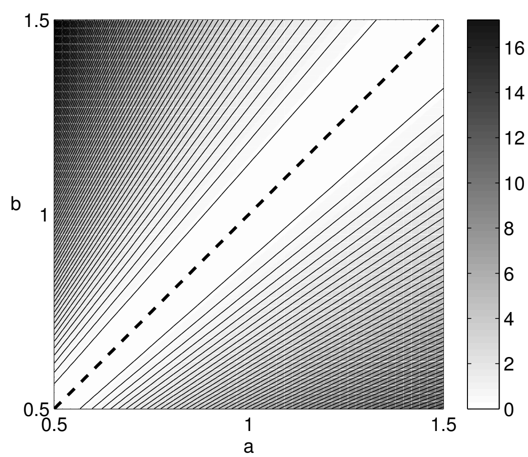

Figure 2: Level curves of the error function ψ^1 when all the elastances are multiplied by a and all the resistances are multiplied by b. The dotted line is the curve $a = b$.

3.2. Output set containing only pressures

Once again, from the model equations, it can be seen that all simulated pressures will be exactly the same if all elastances (E_{ao}, E_{vc}, E_{pa}, E_{pu}, E_{lv} and E_{rv}) and resistances (R_{sys}, R_{pul}, R_{mt}, R_{av}, R_{tc}, R_{pv}) are multiplied by the same factor, while SBV is divided by this factor. For illustration, Figure 3 shows that the error function ψ^2 is equal to zero all along the curve $c = 1/d$, where c is a factor multiplying all the elastances and resistances and d is the one multiplying SBV.

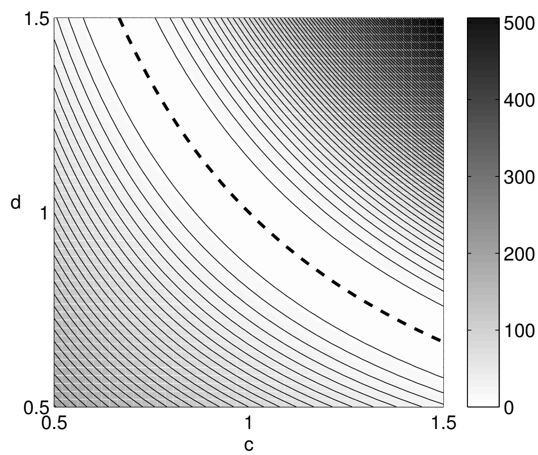

Figure 3: Level curves of the error function ψ^2 when all the elastances and resistances are multiplied by c and SBV is multiplied by d. The dotted line is the curve $c = 1/d$.

3.3. Clinically available output set

It can be shown that all thirteen parameters of the six-chamber CVS model can be uniquely retrieved from the output set $\mathbf{y}^3$. The corresponding demonstration is quite technical and is provided in the following section. This outcome, in turn, proves that the six-chamber CVS model is structurally globally identifiable from these output signals. Consequently, given all required measurements of the outputs, there exists one and only one possible parameter set corresponding to these measurements.

The error function ψ^3 thus possesses a unique global minimum. Figures 4 and 5 confirm that when the output set $\mathbf{y}^3$ is selected, the two indeterminations of Figures 2 and 3 do not occur and the error function ψ^3 has a single minimum.

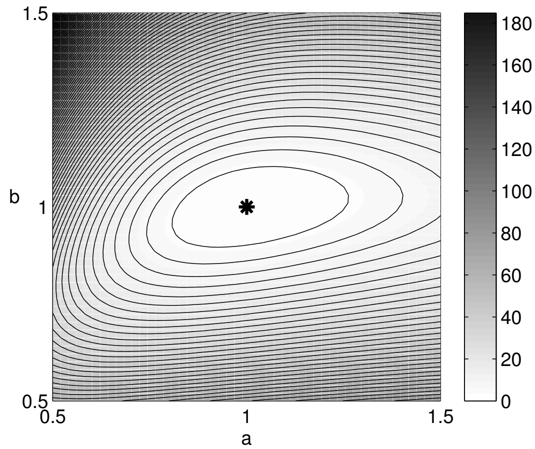

Figure 4: Level curves of the error function ψ^3 when all the elastances are multiplied by a and all the resistances are multiplied by b.

3.4. Demonstration of structural identifiability from the third output set

To perform the structural identifiability analysis of a model, it is assumed that the outputs can be perfectly and continuously measured [20]. Consequently, they can be differentiated as much as necessary. As a reminder, the outputs of the six-chamber model are chosen to be:

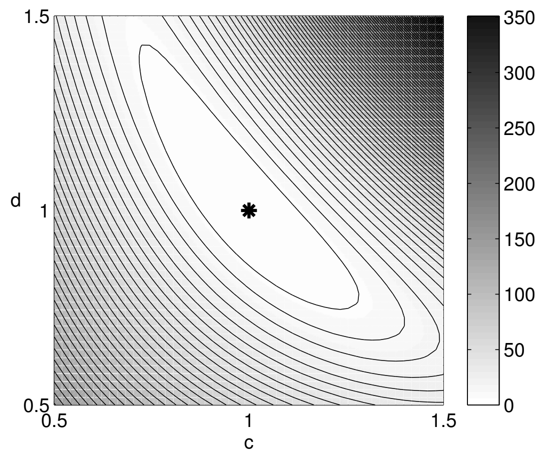

Figure 5: Level curves of the error function ψ^3 when all the elastances and resistances are multiplied by c and SBV is multiplied by d.

- pressure in the aorta $P_{ao}(t)$,
- pressure in the pulmonary artery $P_{pa}(t)$,
- pressure in the vena cava $P_{vc}(t)$,
- pressure in the pulmonary veins $P_{pu}(t)$ and
- stroke volume SV.

Furthermore, it will also be assumed that the left and right driver functions $e_{lv}(t)$ and $e_{rv}(t)$ are known.

In the following sections, it is shown that unique relationships can be established between the thirteen model parameters in $\mathbf{p}$ and the five previously mentioned model outputs in $\mathbf{y}^3$. This outcome implies that the six-chamber model is identifiable from this output set.

3.4.1. During the whole cardiac cycle

Integrating Equation (7) over a whole heart beat from 0 to one cardiac period T yields:

$$\int_0^T Q_{sys}(t)\ dt = \frac{\int_0^T [P_{ao}(t) - P_{vc}(t)]\ dt}{R_{sys}}. \tag{29}$$

Rearranging this equation gives:

$$R_{sys} = \frac{\int_0^T P_{ao}(t)\ dt - \int_0^T P_{vc}(t)\ dt}{\int_0^T Q_{sys}(t)\ dt}. \tag{30}$$

This actually corresponds to the medical definition of systemic vascular resistance [21].

During a whole cardiac cycle, all blood ejected by the heart, *i.e.* the stroke volume, flows through the systemic circulation:

$$\int_0^T Q_{sys}(t)\ dt = \mathrm{SV}. \tag{31}$$

Using Equations (30) and (31) then gives:

$$R_{sys} = \frac{\int_0^T P_{ao}(t)\ dt - \int_0^T P_{vc}(t)\ dt}{\mathrm{SV}}. \tag{32}$$

Equation (32) makes it possible to compute R_{sys}, since all elements of the right-hand side are known. This can also be applied to the pulmonary circulation, thus proving the identifiability of R_{pul}.

3.4.2. During ejection

When the aortic valve opens (t_{AVO}), left ventricular pressure equals aortic pressure:

$$P_{ao}(t_{AVO}) = P_{lv}(t_{AVO}) \tag{33}$$

Using Equation (5) gives:

$$\begin{aligned} P_{ao}(t_{AVO}) &= E_{lv} \cdot e_{lv}(t_{AVO}) \cdot V_{lv}(t_{AVO}) \\ \Leftrightarrow V_{lv}(t_{AVO}) &= \tfrac{P_{ao}(t_{AVO})}{E_{lv} \cdot e_{lv}(t_{AVO})}. \end{aligned} \tag{34}$$

This last quantity is the end-diastolic volume. Similarly, at the time of aortic valve closing (t_{AVC}), left ventricular pressure once again equals aortic pressure:

$$\begin{aligned} P_{ao}(t_{AVC}) &= P_{lv}(t_{AVC}) \\ &= E_{lv} \cdot e_{lv}(t_{AVC}) \cdot V_{lv}(t_{AVC}) \\ \Leftrightarrow V_{lv}(t_{AVC}) &= \tfrac{P_{ao}(t_{AVC})}{E_{lv} \cdot e_{lv}(t_{AVC})}. \end{aligned} \tag{35}$$

This is the end-systolic volume. By definition, the stroke volume SV is equal to the difference between the end-diastolic and end-systolic volumes:

$$\begin{aligned} \mathrm{SV} &= V_{lv}(t_{AVO}) - V_{lv}(t_{AVC}) \\ &= \tfrac{1}{E_{lv}} \left(\tfrac{P_{ao}(t_{AVO})}{e_{lv}(t_{AVO})} - \tfrac{P_{ao}(t_{AVC})}{e_{lv}(t_{AVC})} \right) \end{aligned} \tag{36}$$

$$\Leftrightarrow E_{lv} = \frac{1}{\mathrm{SV}} \left(\frac{P_{ao}(t_{AVO})}{e_{lv}(t_{AVO})} - \frac{P_{ao}(t_{AVC})}{e_{lv}(t_{AVC})} \right) \tag{37}$$

which provides the third identified parameter E_{lv}. The right ventricular end-systolic elastance E_{rv} is identifiable using the right ventricular counterpart of Equation (37).

During cardiac ejection, right ventricular pressure is higher than vena cava pressure ($P_{rv}(t) > P_{vc}(t)$). Consequently, the combination of Equations (7), (11) and (15) can be written:

$$\dot{V}_{vc}(t) = Q_{sys}(t) = \frac{P_{ao}(t) - P_{vc}(t)}{R_{sys}}. \tag{38}$$

Combining this equation with Equation (2) gives:

$$\dot{P}_{vc}(t) = E_{vc} \cdot \frac{P_{ao}(t) - P_{vc}(t)}{R_{sys}}. \tag{39}$$

The previous equation shows that E_{vc} can be identified:

$$E_{vc} = \frac{\dot{P}_{vc}(t) \cdot R_{sys}}{P_{ao}(t) - P_{vc}(t)}. \tag{40}$$

Since the data is assumed to be perfect, the right-hand side of Equation (40) is exactly equal to E_{vc} at any time during cardiac ejection.

The reasoning that has been exposed for the systemic circulation can be transposed to the pulmonary side. Consequently, pulmonary vein elastance E_{pu} can be obtained using the counterpart of Equation (40).

3.4.3. During filling

Focusing now on (left) ventricular filling ($P_{ao}(t) > P_{lv}(t)$), the combination of Equations (7), (10) and (14) gives:

$$\dot{V}_{ao}(t) = -Q_{sys}(t) = -\frac{P_{ao}(t) - P_{vc}(t)}{R_{sys}}. \tag{41}$$

Using Equation (1), Equation (41) becomes:

$$\dot{P}_{ao}(t) = -E_{ao} \cdot \frac{P_{ao}(t) - P_{vc}(t)}{R_{sys}}. \tag{42}$$

This equation can be solved for E_{ao}, proving that this parameter is identifiable:

$$E_{ao} = -\frac{\dot{P}_{ao}(t) \cdot R_{sys}}{P_{ao}(t) - P_{vc}(t)}. \tag{43}$$

Since the data is assumed to be perfect, the right-hand side of Equation (43) is exactly equal to E_{ao} at any time during ventricular filling. The same reasoning applies to the right ventricular filing, hence providing the value of E_{pa}, which will be used further in this demonstration.

During right ventricular filling ($P_{vc}(t) > P_{rv}(t)$), flow through the tricuspid valve is not zero. The combination of Equations (2), (7), (11) and (15) yields:

$$\dot{P}_{vc}(t) = E_{vc} \left(\frac{P_{ao}(t) - P_{vc}(t)}{R_{sys}} - \frac{P_{vc}(t) - P_{rv}(t)}{R_{tc}} \right). \tag{44}$$

If Equation (44) is differentiated once more, the result is:

$$\ddot{P}_{vc}(t) = E_{vc} \left(\frac{\dot{P}_{ao}(t) - \dot{P}_{vc}(t)}{R_{sys}} - \frac{\dot{P}_{vc}(t) - \dot{P}_{rv}(t)}{R_{tc}} \right). \tag{45}$$

To eliminate $\dot{P}_{rv}(t)$, the derivative of Equation (6) can be used:

$$\dot{P}_{rv}(t) = E_{rv} \cdot \dot{e}_{rv}(t) \cdot V_{rv}(t) + E_{rv} \cdot e_{rv}(t) \cdot \dot{V}_{rv}(t). \tag{46}$$

To eliminate $\dot{V}_{rv}(t)$, the combination of Equations (11), (12) and (16) during filling yields:

$$\dot{V}_{rv}(t) = \frac{P_{vc}(t) - P_{rv}(t)}{R_{tc}}. \tag{47}$$

The algebraic system formed by Equations (6), (44), (45), (46) and (47) counts five equations and five unknowns R_{tc}, $P_{rv}(t)$, $V_{rv}(t)$, $\dot{P}_{rv}(t)$, $\dot{V}_{rv}(t)$. Solving this system with a symbolic computation software (Mathematica Version 8.0, Wolfram Research, Inc., Champaign, IL) shows that it has a unique solution at each instant. The uniqueness of the solution, in turn, guarantees the identifiability of the parameter R_{tc}. It also provides the curve of $V_{rv}(t)$ during filling, which will be useful further in this demonstration. The approach applied here can be repeated with the other side of the circulation to prove the identifiability of the mitral valve resistance R_{mt} and the availability of the left ventricular volume curve $V_{lv}(t)$ during filling.

Since arterial and venous pressures are known, as well as the elastances of the four corresponding chambers (E_{ao}, E_{vc}, E_{pa} and E_{pu}), stressed volume in these chambers can be obtained from Equations (1) to (4). And, since ventricular volumes $V_{lv}(t)$ and $V_{rv}(t)$ are now also known, SBV can be computed from its definition (Equation (20)):

$$\begin{aligned} \text{SBV} = \quad & V_{lv}(t) + \tfrac{P_{ao}(t)}{E_{ao}} + \tfrac{P_{vc}(t)}{E_{vc}} \\ & + V_{rv}(t) + \tfrac{P_{pa}(t)}{E_{pa}} + \tfrac{P_{pu}(t)}{E_{pu}}. \end{aligned} \tag{48}$$

3.4.4. During ejection (bis)

The knowledge of the aortic elastance E_{ao} from the previous section now makes it possible to obtain the value of the aortic valve resistance R_{av}. To do so, it is necessary to return to the ejection phase and to apply a similar reasoning as the one used to compute the tricuspid valve resistance R_{tc}. During left ventricular ejection ($P_{lv}(t) > P_{ao}(t)$), flow through the aortic valve is not zero. The combination of Equations (1), (7), (10) and (14) now yields:

$$\dot{P}_{ao}(t) = E_{ao}\left(\frac{P_{lv}(t) - P_{ao}(t)}{R_{av}} - \frac{P_{ao}(t) - P_{vc}(t)}{R_{sys}}\right). \tag{49}$$

If Equation (49) is differentiated once more, the result is:

$$\ddot{P}_{ao}(t) = E_{ao}\left(\frac{\dot{P}_{lv}(t) - \dot{P}_{ao}(t)}{R_{av}} - \frac{\dot{P}_{ao}(t) - \dot{P}_{vc}(t)}{R_{sys}}\right). \tag{50}$$

To eliminate $\dot{P}_{lv}(t)$, the derivative of Equation (5) can be used:

$$\dot{P}_{lv}(t) = E_{lv} \cdot \dot{e}_{lv}(t) \cdot V_{lv}(t) + E_{lv} \cdot e_{lv}(t) \cdot \dot{V}_{lv}(t). \tag{51}$$

To eliminate $\dot{V}_{lv}(t)$, the combination of Equations (9), (10) and (13) during ejection yields:

$$\dot{V}_{lv}(t) = -\frac{P_{lv}(t) - P_{ao}(t)}{R_{av}}. \tag{52}$$

The algebraic system formed by Equations (5), (49), (50), (51) and (52) counts five equations and five unknowns R_{av}, $P_{lv}(t)$, $V_{lv}(t)$, $\dot{P}_{lv}(t)$, $\dot{V}_{lv}(t)$. Solving this system shows that it has a unique solution at each instant. This outcome, in turn, guarantees the identifiability of the parameter R_{av}. The parameter R_{pv} can also be computed using the same manipulation on the right ventricle and pulmonary artery.

All thirteen model parameters have thus been shown to be computable from the selected set of model outputs, which implies that the six-chamber CVS model is structurally globally identifiable from this set of model outputs. For a better understanding, the demonstration exposed above is summarized in Table 1. Each model parameter involved is linked with the equation(s) used to compute it from the output set $\mathbf{y}^3$.

4. Discussion

The aim of this work was to investigate the structural identifiability of a lumped-parameter CVS model, from three different output sets. The property of being structurally identifiable guarantees that all model parameters can be uniquely retrieved under the assumption of perfect measurements of the outputs. If a model cannot be shown to be structurally identifiable, performing parameter identification using real data is risky, because there is no guarantee that the resulting parameter values are unique.

The first output set $\mathbf{y}^1$ contained volumes in all six model chambers and using it resulted in a case of structural non-identifiability. Two conclusions

Parameter	**Corresponding Equation(s)**
R_{sys}	(32)
R_{pul}	(32)*
E_{lv}	(37)
E_{rv}	(37)*
E_{vc}	(40)
E_{pu}	(40)*
E_{ao}	(43)
E_{pa}	(43)*
R_{tc}	(6), (44), (45), (46) and (47)
R_{mt}	(5), (44)*, (45)*, (46)* and (47)*
SBV	(48)
R_{av}	(5), (49), (50), (51) and (52)
R_{pv}	(6), (49)*, (50)*, (51)* and (52)*

Table 1: Summary of the demonstration of structural identifiability of the six-chamber CVS model. The asterisk (*) denotes the right or pulmonary circulation counterpart of an equation.

can be derived from this result. First, the model will also be structurally non-identifiable from any output set that is a subset of $\mathbf{y}^1$, *i.e.* that contains only volumes in part of the model chambers. Second, it can be stated that a good output set for this CVS model has to contain more information than only volumes.

Similarly, the second output set $\mathbf{y}^2$ contained pressures in all six model chambers and also resulted in a case of structural non-identifiability. This second result implies that the model will also be non-identifiable from an output set containing only pressures in part of the model chambers and that a good output set for this CVS model must include more information than only pressures.

Taking these two observations together results in the conclusion that a good output set for this CVS model must combine information on both pressures and volumes for the model to stand a chance to be structurally identifiable. However, due to the lumped nature of the model and technical limitations, chamber volumes are actually very difficult to measure. Hence, only one (unavoidable) volume measurement, stroke volume, was included in the third output set $\mathbf{y}^3$. The rest of the set consisted of arterial and venous pressures, both on the systemic and pulmonary sides. The model was then showed to be structurally identifiable from this output set.

Plots of the error function associated to the third output set helped illustrate that the non-identifiability cases vanished for this output set. However, the plots of Figures 4 and 5 do not constitute by themselves a demonstration of identifiability. To demonstrate identifiability from plots of the error function would require the impossible task of plotting the 13-dimensional error function for all parameter values. This is the reason why the mathematical demonstration of Section 3.4 was performed.

The measurements contained in $\mathbf{y}^3$ can easily be obtained in an intensive care unit setting. First, stroke volume is generally determined using transpulmonary thermodilution techniques [22]. Second, systemic arterial pressure and vena cava pressure can be obtained using arterial and central venous lines [9]. Finally, pulmonary arterial and venous pressures can be measured using a pulmonary occlusion catheter, which is the most invasive of these instruments [23].

The six-chamber CVS model was thus shown to be structurally globally identifiable from a limited output set containing arterial and venous pressures and stroke volume. However, this limited measurement set might still be reduced. It would thus be useful to investigate the structural identifiability of all model parameters from other output sets, either smaller or containing different outputs.

To reduce the number of model outputs, additional assumptions may be suitable. For instance, these assumptions can take the form of the definition of a relation between parameters. Another way to reduce the size of the output set is to fix some model parameters to population values. For instance, valve resistances R_{mt}, R_{av}, R_{tc} and R_{pv} were observed to have a bad practical identifiability [8, 24]. A second demonstration, performed in Appendix A, shows that, if valve resistances are not identified, the remaining parameters can be identified using an output set $\mathbf{y}^4$ containing only aortic pressure $P_{ao}(t)$, pulmonary artery pressure $P_{pa}(t)$ and stroke volume SV. In this case, venous pressures $P_{vc}(t)$ and $P_{pu}(t)$ do not have to be included in the outputs, which is a significant improvement. Fortunately, valve resistances might be determined *a priori* as population constants based on experimental tests or anthropomorphic data.

It is also important to mention that, even if the present analysis was focused on a particular CVS model, the two non-identifiability cases mentioned in Section 3 are not exclusive to the model of Burkhoff and Tyberg. Many other CVS models suffer the same non-identifiability cases, since they involve very similar equations.

The demonstration presented in Section 3.4 is based on the equations of the present model, and thus, cannot be applied as such to other CVS models. However, most CVS models are built from elements similar to those involved in the model of Burkhoff and Tyberg, for instance time-varying elastances (Equations (5) and (6)) and vascular resistances (Equations (7) and (8)). Consequently, Equations (32) and (37), that were developed to show the identifiability of these parameters, can be used with other models.

5. Conclusions

The six-chamber CVS model of Burkhoff and Tyberg [3] has been used to track the evolution of diseases in animal experiments [5–7]. However, this CVS model (and others) are not identifiable from any output set. In this work, two such cases of structural non-identifiability have first been presented. These cases occur when the model output set only contains a single type of information (pressure or volume).

Thus, a specific output set was chosen mixing pressure and volume information and containing only a limited number of clinically available measurements. Then, by manipulating the model equations involving these outputs, it was demonstrated that the six-chamber CVS model is structurally globally identifiable. This means that the model parameters are unique and can theoretically be identified from the specified limited output set.

A further simplification was made, assuming known cardiac valve resistances. Because of the poor practical identifiability of these four parameters, this assumption is usual. Under this hypothesis, the six-chamber CVS model is structurally identifiable from an even smaller dataset involving only aortic pressure, pulmonary artery pressure and stroke volume.

The results of this work imply that parameter values computed from limited but well-chosen datasets are theoretically unique. As a consequence, the parameter identification procedure can theoretically be performed on the model from such a well-chosen dataset. The model is thus fully suitable to be used for diagnosis.

6. Acknowledgements

This work was supported by the French Community of Belgium (Actions de Recherches Concertées - Académie Wallonie-Europe), the Belgian Funds for Scientific Research (F.R.S.-FNRS) and EU Marie Curie Actions (FP7-PEOPLE-2012-IRSES).

None of the authors has any conflict of interest to declare.

No ethical approval was required for this study.

7. References

[1] P. J. Hunter, A. J. Pullan, B. H. Smaill, Modeling total heart function, Annual Review of Biomedical Engineering 5 (1) (2003) 147–177.

[2] J.-J. Wang, A. B. O'Brien, N. G. Shrive, K. H. Parker, J. V. Tyberg, Time-domain representation of ventricular-arterial coupling as a windkessel and wave system, American Journal of Physiology - Heart and Circulatory Physiology 284 (4) (2003) H1358–H1368.

[3] D. Burkhoff, J. V. Tyberg, Why does pulmonary venous pressure rise after onset of lv dysfunction: a theoretical analysis, American Journal of Physiology-Heart and Circulatory Physiology 265 (5) (1993) H1819–H1828.

[4] W. P. Santamore, D. Burkhoff, Hemodynamic consequences of ventricular interaction as assessed by model analysis, Am J Physiol 260 (Suppl 1) (1991) H146–H157.

[5] J. A. Revie, D. Stevenson, J. G. Chase, C. J. Pretty, B. C. Lambermont, A. Ghuysen, P. Kolh, G. M. Shaw, T. Desaive, Evaluation of a model-based hemodynamic monitoring method in a porcine study of septic shock, Computational and mathematical methods in medicine 2013.

[6] J. A. Revie, D. J. Stevenson, J. G. Chase, C. E. Hann, B. C. Lambermont, A. Ghuysen, P. Kolh, P. Morimont, G. M. Shaw, T. Desaive, Clinical detection and monitoring of acute pulmonary embolism: proof of concept of a computer-based method, Annals of intensive care 1 (1) (2011a) 1–12.

[7] C. Starfinger, C. E. Hann, J. G. Chase, T. Desaive, A. Ghuysen, G. M. Shaw, Model-based cardiac diagnosis of pulmonary embolism, Computer methods and programs in biomedicine 87 (1) (2007) 46–60.

[8] A. Pironet, T. Desaive, J. G. Chase, P. Morimont, P. C. Dauby, Model-based computation of total stressed blood volume from a preload reduction manoeuvre, Mathematical Biosciences 265 (2015) 28–39.

[9] J. J. Maas, M. R. Pinsky, L. P. Aarts, J. R. Jansen, Bedside assessment of total systemic vascular compliance, stressed volume, and cardiac function curves in intensive care unit patients, Anesthesia & Analgesia 115 (4) (2012) 880–887.

[10] A. Pironet, T. Desaive, S. Kosta, A. Lucas, S. Paeme, A. Collet, C. G. Pretty, P. Kolh, P. C. Dauby, et al., A multi-scale cardiovascular system model can account for the load-dependence of the end-systolic pressure-volume relationship., Biomedical engineering online 12 (1) (2013) 8.

[11] B. W. Smith, J. G. Chase, R. I. Nokes, G. M. Shaw, G. Wake, Minimal haemodynamic system model including ventricular interaction and valve dynamics, Medical engineering & physics 26 (2) (2004) 131–139.

[12] W. van Meurs, Modeling and Simulation in Biomedical Engineering: Applications in Cardiorespiratory Physiology, McGraw-Hill Professional, 2011.

[13] C. Starfinger, J. Chase, C. Hann, G. Shaw, P. Lambert, B. Smith, E. Sloth, A. Larsson, S. Andreassen, S. Rees, Prediction of hemodynamic changes towards PEEP titrations at different volemic levels using a minimal cardiovascular model, Computer Methods and Programs in Biomedicine 91 (2) (2008) 128–134.

[14] J. A. Revie, Model-based cardiovascular monitoring in critical care for improved diagnosis of cardiac dysfunction, Ph.D. thesis, University of Canterbury (2012).

[15] É. Walter, L. Pronzato, Identification of parametric models from experimental data, Communications and Control Engineering, Springer, 1997.

[16] L. Ljung, System identification: theory for the user, P T R Prentice Hall, 1987.

[17] P. Docherty, J. G. Chase, T. Lotz, T. Desaive, A graphical method for practical and informative identifiability analyses of physiological models: A case study of insulin kinetics and sensitivity, BioMedical Engineering OnLine 10 (1) (2011) 39.

[18] H. Suga, K. Sagawa, Instantaneous pressure-volume relationships and their ratio in the excised, supported canine left ventricle, Circulation Research 35 (1) (1974) 117–126.

[19] D. Stevenson, J. Revie, J. G. Chase, C. Hann, G. Shaw, B. Lambermont, A. Ghuysen, P. Kolh, T. Desaive, Beat-to-beat estimation of the continuous left and right cardiac elastance from metrics commonly available in clinical settings, BioMedical Engineering OnLine 11 (1) (2012) 73.

[20] H. Pohjanpalo, System identifiability based on the power series expansion of the solution, Mathematical Biosciences 41 (12) (1978) 21 – 33.

[21] R. Klabunde, A. Dalley, Cardiovascular physiology concepts, Lippincott Williams & Wilkins, 2004.

[22] C. Hofhuizen, B. Lansdorp, J. G. van der Hoeven, G.-J. Scheffer, J. Lemson, Validation of noninvasive pulse contour cardiac output using finger arterial pressure in cardiac surgery patients requiring fluid therapy, Journal of Critical Care 29 (1) (2014) 161 – 165.

[23] K. Abe, T. Mashimo, I. Yoshiya, Arterial oxygenation and shunt fraction during one-lung ventilation: a comparison of isoflurane and sevoflurane, Anesthesia & Analgesia 86 (6) (1998) 1266–1270.

[24] J. A. Revie, D. J. Stevenson, J. G. Chase, C. E. Hann, B. C. Lambermont, A. Ghuysen, P. Kolh, G. M. Shaw, S. Heldmann, T. Desaive, Validation of subject-specific cardiovascular system models from porcine measurements, Computer Methods and Programs in Biomedicine 109 (2) (2013) 197 – 210, Control 2010 Special Edition.

Appendix A. Demonstration of structural identifiability from the fourth output set

In this section, identifiability of the six-chamber is demonstrated from a further reduced output set $\mathbf{y}^4$. To do so, a simplifying hypothesis is necessary, assuming known valve resistances. Thus, R_{mt}, R_{av}, R_{tc} and R_{pv} are assumed known and are not part of the parameter set. The reduced output set used here contains:

- pressure in the aorta $P_{ao}(t)$,
- pressure in the pulmonary artery $P_{pa}(t)$ and
- stroke volume SV.

In particular, this output set does not contain venous pressures. Left and right driver functions $e_{lv}(t)$ and $e_{rv}(t)$ are still assumed known.

Appendix A.1. During Ejection

The reasoning presented in 3.4.2 to obtain Equation (37) expressing E_{lv} in terms of $P_{ao}(t)$, $e_{lv}(t)$ and SV can be repeated here, since all these outputs are known. Left ventricular end-systolic elastance E_{lv} is thus obtained using Equation (37).

During cardiac ejection, left ventricular pressure is higher than aortic pressure ($P_{lv}(t) > P_{ao}(t)$) and pulmonary vein pressure ($P_{lv}(t) > P_{pu}(t)$). Consequently, the combination of Equations (9), (10) and (13) can be written:

$$\dot{V}_{lv}(t) = -\frac{P_{lv}(t) - P_{ao}(t)}{R_{av}} \tag{A.1}$$

Combining this equation with Equation (5) gives:

$$\dot{V}_{lv}(t) = -\frac{e_{lv}(t) \cdot E_{lv} \cdot V_{lv}(t) - P_{ao}(t)}{R_{av}} \tag{A.2}$$

Since $P_{ao}(t)$, E_{lv}, $e_{lv}(t)$ and R_{av} are known, this linear differential equation with variable coefficients can be solved for $V_{lv}(t)$ (during cardiac ejection). The initial condition required for solving is obtained from Equation (34). Once $V_{lv}(t)$ is known, $P_{lv}(t)$ during ejection can be computed using Equation (5). It will be used further in the demonstration.

During ejection, the combination of Equations (7), (10) and (14) gives:

$$\dot{V}_{ao}(t) = \frac{P_{lv}(t) - P_{ao}(t)}{R_{av}} - \frac{P_{ao}(t) - P_{vc}(t)}{R_{sys}}. \tag{A.3}$$

Multiplying both sides of this equation by E_{ao} and using the fact that $P_{ao}(t) = E_{ao} \cdot V_{ao}(t)$ yields:

$$\dot{P}_{ao}(t) = \frac{E_{ao}}{R_{av}}(P_{lv}(t) - P_{ao}(t)) - \frac{E_{ao}}{R_{sys}}(P_{ao}(t) - P_{vc}(t)). \tag{A.4}$$

Differentiating this equation with respect to time then results in:

$$\ddot{P}_{ao}(t) = \frac{E_{ao}}{R_{av}}(\dot{P}_{lv}(t) - \dot{P}_{ao}(t)) - \frac{E_{ao}}{R_{sys}}(\dot{P}_{ao}(t) - \dot{P}_{vc}(t)). \tag{A.5}$$

Then, taking into account that $P_{rv}(t) > P_{vc}(t)$ during ejection, Equations (2), (7), (11) and (15), can be used to substitute $\dot{P}_{vc}(t)$:

$$\begin{aligned} \ddot{P}_{ao}(t) = \quad & \tfrac{E_{ao}}{R_{av}}(\dot{P}_{lv}(t) - \dot{P}_{ao}(t)) \\ & -\tfrac{E_{ao}}{R_{sys}}\left(\dot{P}_{ao}(t) - \tfrac{E_{vc}}{R_{sys}}(P_{ao}(t) - P_{vc}(t))\right). \end{aligned} \tag{A.6}$$

The same two steps can be repeated twice to obtain the following two equations:

$$\begin{aligned} P_{ao}^{(3)}(t) = \quad & \tfrac{E_{ao}}{R_{av}}(\ddot{P}_{lv}(t) - \ddot{P}_{ao}(t)) \\ & -\tfrac{E_{ao}}{R_{sys}} \cdot \ddot{P}_{ao}(t) \\ & +\tfrac{E_{ao} \cdot E_{vc}}{R_{sys}^2}\left(\dot{P}_{ao}(t) - \tfrac{E_{vc}}{R_{sys}}(P_{ao}(t) - P_{vc}(t))\right) \end{aligned} \tag{A.7}$$

$$\begin{aligned} P_{ao}^{(4)}(t) = \quad & \tfrac{E_{ao}}{R_{av}}(P_{lv}^{(3)}(t) - P_{ao}^{(3)}(t)) \\ & -\tfrac{E_{ao}}{R_{sys}} P_{ao}^{(3)}(t) \\ & +\tfrac{E_{ao} \cdot E_{vc}}{R_{sys}^2} \ddot{P}_{ao}(t) \\ & -\tfrac{E_{ao} \cdot E_{vc}^2}{R_{sys}^3}\left(\dot{P}_{ao}(t) - \tfrac{E_{vc}}{R_{sys}}(P_{ao}(t) - P_{vc}(t))\right). \end{aligned} \tag{A.8}$$

The algebraic system formed by Equations (A.4), (A.6), (A.7) and (A.8) counts four equations and four unknowns $P_{vc}(t)$, R_{sys}, E_{ao} and E_{vc} (since $P_{ao}(t)$

and $P_{lv}(t)$ are known). Solving this system shows that it has a unique solution at each instant. This outcome, in turn, guarantees the identifiability of the three parameters R_{sys}, E_{ao} and E_{vc}. It also provides the time course of $P_{vc}(t)$ during ejection.

The reasoning that has been presented in this section can be extended to the right side of the circulation, thus proving the identifiability of parameters E_{rv}, R_{pul}, E_{pa} and E_{pu}.

Appendix A.2. During Isovolumic Contraction and Ejection

During isovolumic contraction and ejection, the mitral and triscuspid valves are closed. Hence, $Q_{mt}(t) = Q_{tc}(t) = 0$. Combining Equations (7), (11) and (15) during this period gives:

$$\dot{V}_{vc}(t) = \frac{P_{ao}(t) - E_{vc} \cdot V_{vc}(t)}{R_{sys}}. \tag{A.9}$$

This linear differential equation with variable coefficients can be solved for $V_{vc}(t)$, since $P_{ao}(t)$, E_{vc} and R_{sys} are now known. To obtain the required initial condition, a series of further manipulations is performed. First, at the time of tricuspid valve closing, vena cava pressure equals right ventricular pressure:

$$P_{vc}(t_{TVC}) = P_{rv}(t_{TVC}). \tag{A.10}$$

Using Equations (2) and (6) then yields:

$$\begin{aligned} E_{vc} \cdot V_{vc}(t_{TVC}) &= E_{rv} \cdot e_{rv}(t_{TVC}) \cdot V_{rv}(t_{TVC}) \\ \Rightarrow V_{vc}(t_{TVC}) &= \tfrac{E_{rv}}{E_{vc}} \cdot e_{rv}(t_{TVC}) \cdot V_{rv}(t_{TVC}). \end{aligned} \tag{A.11}$$

On the other hand, the right or pulmonary side counterpart of Equation (34) is:

$$V_{rv}(t_{PVO}) = \frac{P_{pa}(t_{PVO})}{E_{rv} \cdot e_{rv}(t_{PVO})} \tag{A.12}$$

where t_{PVO} denotes the time of pulmonary valve opening. Using the fact that right ventricular volume does not change between tricuspid valve closing and pulmonary valve opening ($V_{rv}(t_{TVC}) = V_{rv}(t_{PVO})$) to combine Equations (A.11) and (A.12) finally gives the needed initial condition:

$$V_{vc}(t_{TVC}) = \frac{P_{pa}(t_{PVO})}{E_{vc}} \cdot \frac{e_{rv}(t_{TVC})}{e_{rv}(t_{PVO})}. \tag{A.13}$$

As before, the approach applied here can be transposed to the other side of the circulation, which gives the time course of $V_{pu}(t)$ during right ventricular isovolumic contraction and ejection. Finally, since $V_{lv}(t)$, $P_{ao}(t)$, $V_{vc}(t)$, $V_{rv}(t)$, $P_{pa}(t)$ and $V_{pu}(t)$ are now available during ejection, SBV can be computed from its definition (Equation (20)):

$$\begin{aligned} \text{SBV} = \quad & V_{lv}(t) + \tfrac{P_{ao}(t)}{E_{ao}} + V_{vc}(t) \\ & + V_{rv}(t) + \tfrac{P_{pa}(t)}{E_{pa}} + V_{pu}(t). \end{aligned} \tag{A.14}$$

The 9 model parameters of interest can thus be computed from the restricted set of model outputs $\mathbf{y}^4$. The analysis presented in this section is summarized in Table A.2 for clarity.

Parameter	**Corresponding Equation(s)**
R_{tc}	Known
R_{av}	Known
R_{mt}	Known
R_{pv}	Known
E_{lv}	(37)
R_{sys}	(A.4), (A.6), (A.7) and (A.8)
E_{ao}	(A.4), (A.6), (A.7) and (A.8)
E_{vc}	(A.4), (A.6), (A.7) and (A.8)
E_{rv}	(37)*
R_{pul}	(A.4)*, (A.6)*, (A.7)* and (A.8)*
E_{pa}	(A.4)*, (A.6)*, (A.7)* and (A.8)*
E_{pu}	(A.4)*, (A.6)*, (A.7)* and (A.8)*
SBV	(A.14)

Table A.2: Summary of the demonstration of structural identifiability of the six-chamber CVS model with known valve resistances. The asterisk (*) denotes the right or pulmonary circulation counterpart of an equation.